



Journal of Applied and Computational Mechanics



Research Paper

Random Walk Particle Tracking for Convection-diffusion Dominated Problems in Shallow Water Flows

Hind Talbi¹, Elmiloud Chaabelasri², Mohammed Jeyar³, Najim Salhi⁴

¹ LME, Department of Physics, Faculty of Science, Mohammed First University, 60000 Oujda, Morocco, Email h.talbi@ump.ac.ma

² LPTPME, Department of Physics, Faculty of Science, Mohammed First University, 60000 Oujda, Morocco, Email: e.chaabelasri@ump.ac.ma

³ LME, Department of Physics, Faculty of Science, Mohammed First University, 60000 Oujda, Morocco, Email jeyar.mohammed.88@gmail.com

⁴ LME, Department of Physics, Faculty of Science, Mohammed First University, 60000 Oujda, Morocco, Email: najim.salhi@yahoo.fr

Received September 23 2020; Revised October 29 2020; Accepted for publication October 29 2020.

Corresponding author: Elmiloud Chaabelasri (e.chaabelasri@ump.ac.ma)

© 2020 Published by Shahid Chamran University of Ahvaz

Abstract. This paper deals with a Lagrangian stochastic approach to solve the advection-diffusion equation of a scalar tracer inflow based on random walk particle tracking (RWPT) of a fine number of particles that describe the tracer. The water flow is governed by the shallow water equations that are solved using a finite volume upwinding scheme on a non-structured triangular mesh. Results are presented for two problems, pure advection in a square cavity and pollutant advection in the strait of Gibraltar, that demonstrate the performance, accuracy, and the flexibility of the RWPT method to examine the process of pollutant convection by comparing predictions with those from the Eulerian approach. The Lagrangian approach is shown to have advantages in terms of the high level of simplicity and stability relative to the Eulerian approach.

Keywords: Lagrangian random walk tracking, Shallow water equations, Convection-diffusion equation, Strait of Gibraltar.

1. Introduction

The convection-diffusion of non-reactive pollutants in shallow water flow can be described by the advection-dispersion equation which is a partial differential equation. It is well known that solving the equation often generates non-physical oscillations and/or numerical diffusion in regions where the hyperbolic nature of the equation becomes predominant. There are two main classes of methods for solving this equation employed in the literature. Firstly, Eulerian methods, the advection-dispersion equations are solved on a fixed mesh. The main corresponding numerical methods are Finite volume (VF), Finite difference (DF), finite element (EF). These methods conserve mass and are easy to implement. Secondly, Lagrangian methods, the convection equation is solved using a set of discrete particles that move relative to the fixed frame of reference. All the data and variables that constitute the problem are indexed and linked to each particle.

In this work, we will focus on a Lagrangian method, called random walk particle tracking (RWPT), to simulate the tracer particle motion due to the advection and diffusion processes [1]. The RWPT is based on a deterministic advection process and a stochastic dispersion process to describe the dispersive component of particle displacement [2,3]. Therefore, in water flows the Lagrangian method of the RWPT technique has long been used the analysis of dispersion and diffusion processes for supercritical flow in porous media [4,5]. It employs a band of discrete particles to depict the pollutant plume, and the particles are tracked independently in flows. The RWPT method can typically give a good approximation of the concentration gradients and the numerical calculation can be readily parallelized and without numerical diffusion [6,7]. Consequently, the RWPT method has been used extensively to simulate, on a massive scale, biogeochemical and reactive convection problems [8,9]. In [10] have evolved a successful RWPT approach for the convection of contaminants simulation in media, which takes into consideration discontinuous dispersion coefficients. The authors present improvements to the concept of a partially reflecting barrier used to account for these discontinuities, The authors' new algorithm efficiently simulates both advection- and dispersion-dominated convection conditions, it improves the applicability of RWPT to situations in which both conditions occur. In [11] has also elaborated a model employs the RWPT method for simulation of the two-dimensional contaminant convection process and preserve transport characteristics between the discrete fracture network and the mapped continuum. In this study, the flow problem is solved via MODFLOW and the transport problem is solved on the grid using a particle tracking method. It is found that the proposed technique is useful to preserve conservative transport characteristics on the grid. Several authors have demonstrated that the RWPT technique of solute convection problems by dividing the solute masse into a great number of particles is stable and accurate [12,13]. The interpolation schemes and reflection principle that preserve discontinuities in velocity at material contacts are reviewed by LaBolle et al. in [12], the presented results from simulations of transport in porous media demonstrate the potentialities of the improvements to computing solute transport in two-dimensional heterogeneous porous media. In [13], Masciopinto develops a mathematical model using Navier-Stokes and Darcy-Weisbach's equation for a steady and



non-uniform flow, and particle tracking technique to simulate the transport in fractured rocks. The computational model was used to estimate the mass balance aperture and the tracer aperture. The values they found are consistent with hydraulic apertures, and show a similar trend. In [14] it was shown that the RWPT has been more successful than the Eulerian approach within an unsteady flow. Zhang et al. used, in modeling particle transport and distribution in enclosed spaces, both the Eulerian and Lagrangian models. The two models were further compared in predicting the transient dispersion of the particles from a coughing passenger in a section of airliner cabin. In the unsteady state condition, the Lagrangian method performed better than the Eulerian method. In the same field, Cheng et al. [15] used the random walk method to represent the time-varying directionality of indoor emissions, thereby predicting the time series and frequency distributions of concentrations close to an actively emitting point source. The models were used to estimate the air velocity and the time scale changes of plume stream direction in a typical naturally ventilated residence

The RWP has been extended also for mass convection in depth-averaged flows and much research has demonstrated that the RWPT approach compared with the Eulerian method has achieved higher accuracy in representing pollutant dispersion in depth-averaged flows. Among others, Wu et al. in [16] compared the random walk particle tracking method with the Eulerian methods in investigating pollutant transport in depth-averaged flows in two idealized cases and both numerical results have been compared against the analytical solution. Their simulations by the random walk model achieve higher accuracy in both cases and are free of fictitious oscillations in the vicinity of sharp concentration gradients, unlike the Eulerian method that generates numerical dissipation where concentration changes abruptly. A similar study was conducted by Yang et al. [17], who used a numerical model based on depth-averaged equations and a random walk particle tracking method to solve an instantaneous release problem in uniform flows. In this work, the authors present extensive parametric studies to investigate the influences of the number of particles and the size of time steps. The predictions are found to be independent of time step, but are

to be independent of time steps but are sensitive to the particle numbers. And more recently, Jalali et al. [18] used the coupled shallow flow and particle-tracking model to simulate chaotic advection and mixing processes in a channel containing a pair of side-wall cavities containing a single groyne, and a rectangular channel containing a pair of groynes.

The main concern of this paper is the development of a random walk particle tracking method (RWPT) for convection-diffusion of pollutants in shallow water flow including complex topography on a nonstructural triangular mesh. The shallow water equations are used, to govern the flow, and solved using an upwinding scheme presented in [19,20]. The pollutant mass was divided into finite particles, released, and tracked in the flow using the RWPT method. In this work a conservative algorithm was developed to initialize the particles into the mesh from the pollutant concentration, then, rebuild the concentration from the particle cloud transported in the water flow. A nearest neighbors scheme was used to calculate the Lagrangian velocity.

The layout of this work is as follows. In section 2, we describe our mathematical formulation of the shallow-water equations, and introduce the numerical method applied to solve it. We deliver a brief overview of the Eulerian approach, and with a specific focus of RWPT. Section 3 is devoted to discussing the results of the two problems. Finally, section 4 presents the conclusion reached from our works.

2. Mathematical Models and Numerical Tools

2.1 Eulerian hydrodynamical model

In the context of shallow water flow, the two-dimensional shallow water (SW) equations are used to simulate the hydrodynamical behavior within the considered domain. This model is derived from depth-integrating mass continuity and Navier-Stokes momentum equations under the assumption that vertical pressure gradients are nearly hydrostatic, implying that the horizontal velocity field is constant throughout the depth of the water. In the case where the horizontal length scale is much greater than the vertical length scale, the example of the Strait of Gibraltar, this assumption is widely valid. In a two dimensional Cartesian coordinate system, the continuity and the momentum equations of the SW equations model take the following form:

$$\begin{cases} h_t + (hu)_x + (hv)_y = 0 \\ (hu)_t + \left(hu^2 + \frac{1}{2}gh^2\right)_x + (huv)_y = -gh\left(Z_x - n^2 \frac{u\|u\|}{h^{4/3}}\right) \\ (hu)_t + (huv)_x + \left(hv^2 + \frac{1}{2}gh^2\right)_y = -gh\left(Z_y - n^2 \frac{v\|u\|}{h^{4/3}}\right) \end{cases} \tag{1}$$

where g is the gravitational acceleration, h is the water height, u and v are the mass-flow averaged velocity components in the x and y direction respectively, where Z denotes the bottom topography and n is the Manning roughness coefficient. Note that the indices x , y and t represent spatial and temporal derivatives.

In the existence of convection-diffusion of a passive pollutant in the water flow, i.e. the pollutants do not interact with the water flow, the previous model is enriched by the convection-diffusion equation, integrated over the water height h and solved simultaneously with the SW equations. For the average pollutant concentration C of the water layer h , the following convection-diffusion equation holds:

$$(hC)_t + (huC)_x + (hvC)_y = D((hC_x)_x + (hC_y)_y) \tag{2}$$

where D is an empirical diffusion coefficient. Remark that we have considered only the case of isotropic pollutant diffusion for simplicity. The depth-averaged shallow water equations coupled with the advection-diffusion equation for the depth-averaged pollutant concentration are described by the following system of equations:

$$\begin{bmatrix} h \\ hu \\ hv \\ hC_t \end{bmatrix} + \begin{bmatrix} hu \\ hu^2 + \frac{gh^2}{2} \\ huv \\ huC \end{bmatrix}_x + \begin{bmatrix} hv \\ hv^2 + \frac{gh^2}{2} \\ huv \\ hvC \end{bmatrix}_y = \begin{bmatrix} 0 \\ -gh\left(Z_x - n^2 \frac{u\|u\|}{h^{4/3}}\right) \\ -gh\left(Z_y - n^2 \frac{v\|u\|}{h^{4/3}}\right) \\ D((hC_x)_x + (hC_y)_y) \end{bmatrix} \tag{3}$$



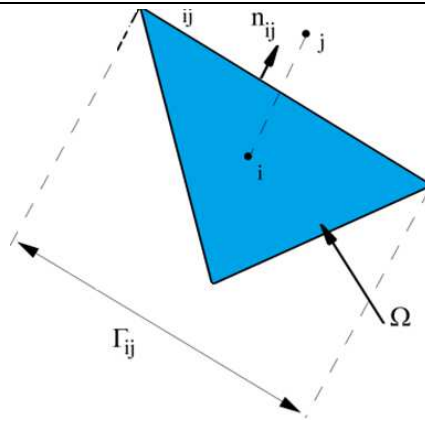


Fig. 1. Unstructured mesh, triangular control volume and notations.

The previous set of equations (3) is a system of strictly hyperbolic non-linear partial differential equations and can be written in a form of homogeneous system as:

$$W_t + F(W)_x + G(W)_y = S(W) \tag{4}$$

To integrate this system under the finite volume assumptions over an unstructured mesh, the flow domain is partitioned into a set of triangular cells or finite volumes. Let ij be the common edge of two neighboring cells i and j , with Γ_{ij} its length, $N(i)$ is the set of neighboring triangles of cell i , and \mathbf{n}_{ij} is the unit vector normal to the edge ij and points toward the cell j (Fig. 1)

Integrating the system (4) in a considering triangular control volume Ω , and invoking the Gauss theorem:

$$\frac{\partial}{\partial t} \int_{\Omega} W d\Omega + \int_{\Omega} \Delta F d\Omega = \int_{\Omega} S d\Omega \Rightarrow \frac{\partial}{\partial t} \int_{\Omega} W d\Omega + \int_{\partial\Omega} (F \cdot \mathbf{n}) d\Omega = \int_{\Omega} S d\Omega \tag{5}$$

Assuming a piecewise constant representation, the integral around an element is approximated as the sum of the numerical flux contributions from each edge, such that

$$\frac{W_i^{n+1} - W_i^n}{\Delta t} V_i + \sum_{j \in N(i)} \delta F_{ij} \Gamma_{ij} = \int_{V_i} S(W_i^n) dV \tag{6}$$

where $W_i^n = W(x_i, t_n)$ is the vector of conserved variables evaluated at time level $t_n = n\Delta t$, n is the number of time steps, Δt is the time step, V_i is the area of cell i , $F = Fn_x + Gn_y$ is normal flux, δF_{ij} is the numerical flux through the edge ij that has a length Γ_{ij} .

Herein, the following upwind scheme based on Roe's approximate Riemann solver is employed to determine the numerical flux on the control volume surfaces. At each cell edge [22],

$$\delta F_{ij} = \frac{1}{2} (F(\bar{W}_i, \mathbf{n}_{ij}) + F(\bar{W}_j, \mathbf{n}_{ij})) - \frac{1}{2} |J(\bar{W}, \mathbf{n}_{ij})| (\bar{W}_j - \bar{W}_i) \tag{7}$$

in which

$$|J(\bar{W}, \mathbf{n}_{ij})| = P(\bar{W}, \hat{\mathbf{n}}_{ij}) |\Lambda(\bar{W}, \mathbf{n}_{ij})| P^{-1}(\bar{W}, \mathbf{n}_{ij}) \tag{8}$$

where $J(\bar{W}, \mathbf{n}_{ij})$ is the flux Jacobian evaluated using Roe's average state \bar{W} :

$$\bar{W} = \left(\frac{h_i + h_j}{2}, \frac{u_i \sqrt{h_i} + u_j \sqrt{h_j}}{\sqrt{h_i} + \sqrt{h_j}} \bar{h}, \frac{v_i \sqrt{h_i} + v_j \sqrt{h_j}}{\sqrt{h_i} + \sqrt{h_j}} \bar{h} \right)^T \tag{9}$$

The normal flux can then be written as

$$\delta F_{ij} = \frac{1}{2} (F(\bar{W}_i, \mathbf{n}_{ij}) + F(\bar{W}_j, \mathbf{n}_{ij})) - \sum_{k=1}^3 \bar{\varphi}_k |\lambda_k| \bar{e}_k \tag{10}$$

where $\bar{\varphi}$ are the wave strengths given by

$$\bar{\varphi}_{1,3} = \frac{1}{2} \Delta h \pm \frac{1}{2c} \bar{h} \Delta u \text{ and } \bar{\varphi}_2 = \bar{h} \Delta v \tag{11}$$

The source terms are balanced by means of a two-dimensional implementation of the upwind scheme proposed by Vazquez



et al. [23,24] for treating the homogeneous part of Saint-Venant equations, and which satisfies the exact conservation C-property. Integration of the source term on the control volume V_i is written,

$$\int_{V_i} \mathbf{S}^n(\mathbf{w})dV = \sum_{j \in N(i)} \int_{\Gamma_{ij}} \mathbf{S}^n(\mathbf{w}, \mathbf{n}_{ij})d\Gamma \tag{12}$$

Following Bermudez [25], this approximation is upwinded and the source term \mathbf{S}^n replaced by a numerical source vector $\boldsymbol{\psi}^n$, such that

$$\int_{\Gamma_{ij}} \mathbf{S}^n(\bar{\mathbf{w}}, \mathbf{n}_{ij})d\Gamma = \delta \mathbf{S}^n(\bar{\mathbf{w}}_i, \bar{\mathbf{w}}_j, \mathbf{n}_{ij})\Gamma_{ij} \tag{13}$$

At each cell interface Γ_{ij} , the contribution of the source term is defined as the projection of the source term vector in the basis of eigenvectors of the Jacobian matrix. Thus the function source term is,

$$\delta \mathbf{S}^n(\bar{\mathbf{w}}_i, \bar{\mathbf{w}}_j, \mathbf{n}_{ij}) = [\mathbf{I} - \mathbf{A}(\bar{\mathbf{w}}, \mathbf{n}_{ij})\mathbf{A}(\bar{\mathbf{w}}, \mathbf{n}_{ij})] \cdot \hat{\mathbf{S}}^n(\mathbf{X}_i, \mathbf{X}_j, \mathbf{W}_i, \mathbf{W}_j, \mathbf{n}_{ij}) \tag{14}$$

where \mathbf{I} is the identity matrix, $\mathbf{A}(\bar{\mathbf{w}}, \mathbf{n}_{ij})$ is the Roe flux Jacobian, and $\hat{\mathbf{S}}^n(\mathbf{X}_i, \mathbf{X}_j, \mathbf{W}_i, \mathbf{W}_j, \mathbf{n}_{ij})$ represents an approximation of the source term on the cell interface Γ_{ij} . Its choice is crucial to obtain accurate results. Using states W_i and W_j , the approximation $\hat{\mathbf{S}}^n$ is defined by [24] as:

$$\hat{\mathbf{S}}^n(\mathbf{X}_i, \mathbf{X}_j, \mathbf{W}_i, \mathbf{W}_j, \mathbf{n}_{ij}) = \begin{bmatrix} 0 \\ g\sqrt{h_i h_j} \frac{(h_i - h_j)}{d_{ij}} n_{ij}^1 \\ g\sqrt{h_i h_j} \frac{(h_i - h_j)}{d_{ij}} n_{ij}^2 \end{bmatrix} \tag{15}$$

2.2 Random walk particle tracking method

The random walk particle method is employed to solve the convection-diffusion processes as governed by the advection-diffusion equation (2). RWPT simulates pollutant advection and diffusion by partitioning the pollutant mass into a large number of representative particles and monitoring their positions as they undergo movement that depends upon the local velocity field and random fluctuations. The movement of the particle is expressed by the Itô-Taylor integration scheme [26,27]. Therefore, An explicit time integration scheme is used to get the new position of each pollutant particle[28,29]

$$x_p(t + \Delta t_{RW}) = x_p(t) + u_p(t)\Delta t_{RW} + dW(t)\sqrt{2D\Delta t_{RW}} \tag{16}$$

where $x_p = (x_p, y_p)$ the Cartesian are coordinates of an arbitrary particle, u_p is the particle velocity calculated using the nearest neighbor Eulerian velocities from the considered particle, and $dW = (dw_x, dw_y)$ is a random vector whose components are sampled from a Gaussian distribution with unit variance and zero mean.

2.2.1 Initial random points distribution

According to the concentration inside a selected triangle Γ_i , the particle positions are set randomly. The particles number is calculated using the following formula:

$$N_p(\Gamma_i) = N_T \frac{C(\Gamma_i)A(\Gamma_i)}{C_T \sum_{i=1}^{N_{de}} \theta(i)A(\Gamma_i)} \tag{17}$$

where $N_T = \sum_{i=1}^{N_{de}} N_p(\Gamma_i)$ is the total number of generated particles, $C_T = \sum_{i=1}^{N_{de}} C(\Gamma_i)$ if the corresponding total concentration, $A(\Gamma_i)$ is the area of the selected triangle and $\theta(i)$ is an indicator function defined as:

$$\theta(i) = \begin{cases} 1 & \text{if } C(\Gamma_i) \neq 0 \\ 0 & \text{otherwise} \end{cases} \tag{18}$$

If a triangle Γ_i is allowed to contains particles, a set of $N_p(\Gamma_i)$ particles are distributed randomly according to the following formula, that gives the initial position coordinates of each particle.



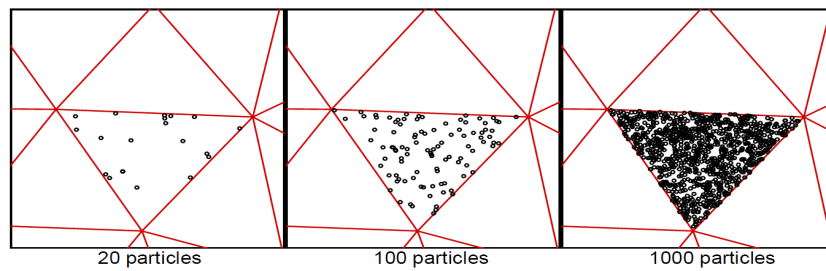


Fig. 2. Examples of initial randomly particles distributed inside a triangle.

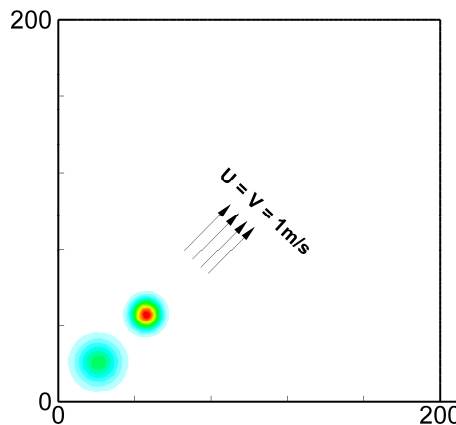


Fig. 3. Domain configuration for the convection in square cavity problem.

$$x_p(t = 0) = \begin{pmatrix} x_i + \frac{2}{3} dw_x \max_{k=1,3} d_k \\ y_i + \frac{2}{3} dw_y \max_{k=1,3} d_k \end{pmatrix} \tag{19}$$

where d_k and (x_i, y_i) are the median length and the barycentre coordinates of the triangle Γ_i . Remark that using the initial particle coordinates formula (19) can generate particles outside the triangle, for that, an iterative particle generator is implemented to validate the particle position before moving to the next triangle. The Fig. 2 gives examples of randomly initial particles according to pollutant concentration inside triangle mesh.

3. Numerical Results

Validation and verification of the RWPT numerical approach were conducted with two tests cited in the literature. The first one concerns an idealized convection of a tracer in a square cavity and the second in the strait of Gibraltar with irregular geometry and bathymetry. Results have been compared with analytical solutions and the Eulerian convection-diffusion equation.

3.1 Convection in a square cavity:

This first problem concerns convection-dominated transport of tracer in a square cavity. The cavity is 20m by 20m. Initially, a tracer, given by a set of particles with concentration $C(x,y,t=0)$ is released in a uniform flow, i.e., $u=v=1m/s$. The initial concentration is given by:

$$C(x, y, t = 0) = c_1 e^{-\frac{(x-x_1)^2+(y-y_1)^2}{\sigma_1}} + c_2 e^{-\frac{(x-x_2)^2+(y-y_2)^2}{\sigma_2}} \tag{20}$$

where (x_1, y_1) and (x_2, y_2) are the initial central coordinates of the tracers and (C_1, C_2) are two constants, here are equal to (0.3,0.7). The profile concentration across the diagonal is given in Fig.4. We included the results of the initial solution, the exact solution, the numerical solutions by the particle tracking method, and the Eulerian convection-diffusion equation. The predictions by the particle tracking method exhibit good agreement with the exact solution. Fig.5 shows the pollutant particles at the initial time $t=0s$ and final time $t=100s$. Fig.6 depicts the final pollutant concentration calculated by RWPT method and the Eulerian Convection-diffusion equation. The analysis of results indicates that the shape of the pollutant plume was preserved along with its convection by the RWPT method, on the contrary of the Eulerian convection-diffusion equation that decreases heavily. We present in Fig.7, the evolution of maximum concentration against the number of triangles obtained using the convection-diffusion equation. It seems that additional mesh refinement does not further improve the results, indicating grid convergence. In all, this numerical test is convincing evidence of the particle tracking method to predict the convection of pollutants by shallow water flow for the pure convection process.

The applicability of the proposed RWPT scheme is also tested against flow over irregular bed. Thus, the previous problem configuration is enhanced by two bumps in the bed (fig. 8). The bed profile is described by the following function:

$$Z(x, y) = e^{-\frac{(x-75)^2+(y-125)^2+(x-125)^2+(y-75)^2}{800}} \tag{21}$$



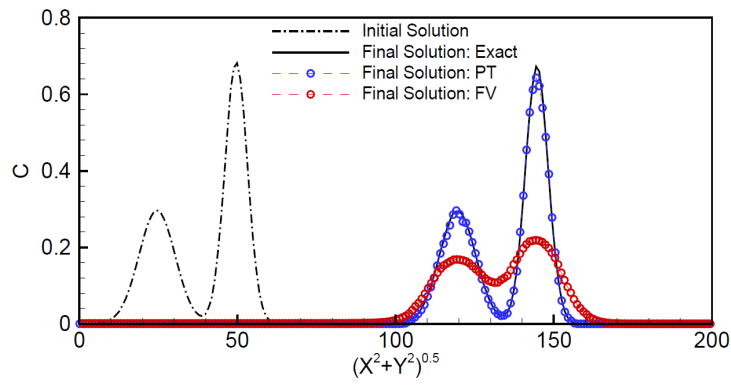


Fig. 4. Cross-section along the diagonal of the initial and final concentration, Results comparison of the particle tracking and Eulerian convection-diffusion equation.

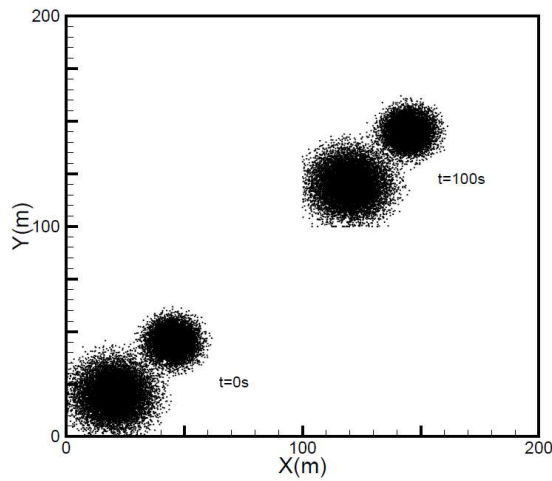


Fig. 5. Screenshot of the particle distribution in their walk at the initial and final time.

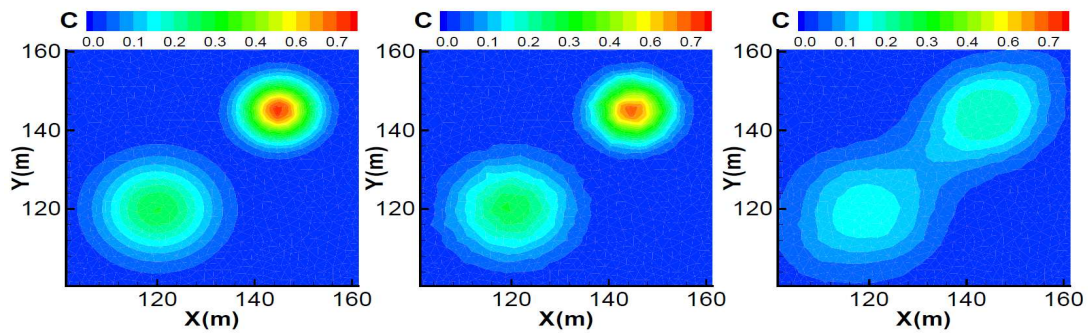


Fig. 6. Zoom in of the two-dimensional final concentration distribution, left: exact solution, middle: Particle tracking method, and right: Eulerian convection-diffusion equation.

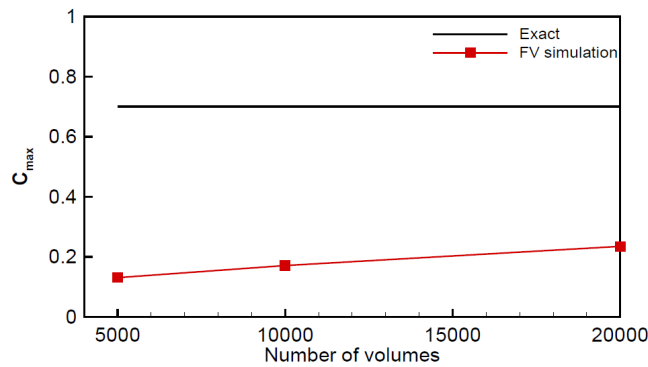


Fig. 7. Evolution of maximum concentration against the number of triangles.



In the present configuration, the same numerical parameters are used except time simulation that is advanced to 150s. The results are presented in terms of pollutant concentration, particle positions, streamlines, and velocity magnitude. Fig.9 shows comparative results for pollutant concentration calculated over the flat and irregular bed and fig.10 presents the flow behavior obtained for the case of irregular bed. The effects of the bed irregularity are shown on the flow, indeed, the streamlines become curved, and the velocity increase near the twin bumps. Accordingly, the particle cloud, displayed in Fig.11, is also affected so that the circular form is deformed. It should be noted that the maximum value is not preserved owing to the diffusion caused by water mixing over the irregular bed.

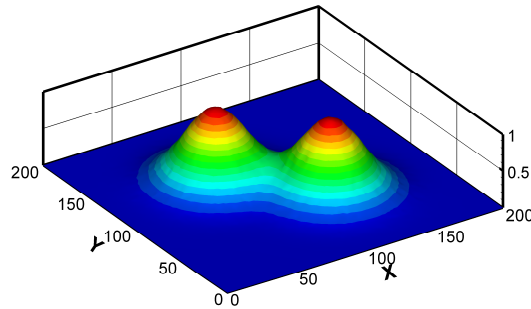


Fig. 8. Bathymetry profile used for the convection in the square cavity over irregular bed.

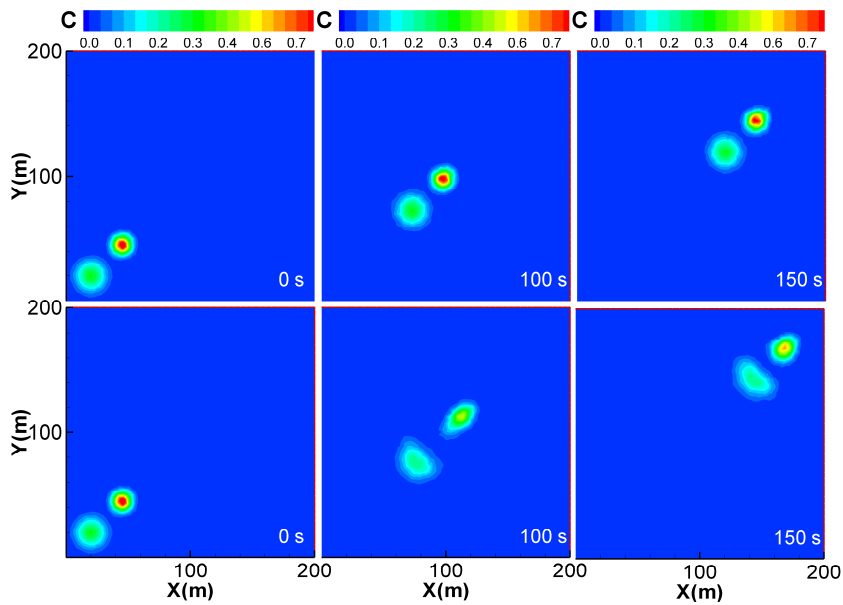


Fig. 9. Pollutant concentration at 0, 100, and 150 s in the case of flat bed (top) and irregular bed (bottom).

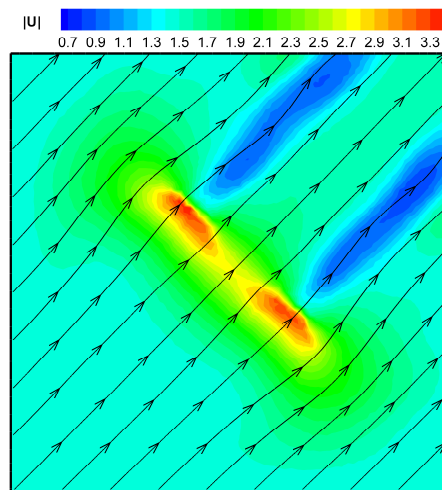


Fig. 10. Streamlines and velocity magnitude of the flow in the case of irregular bed.



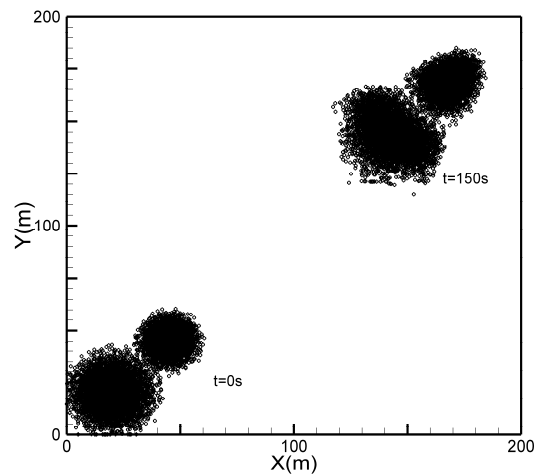


Fig. 11. Particle positions at the initial and final time in case of irregular bed.

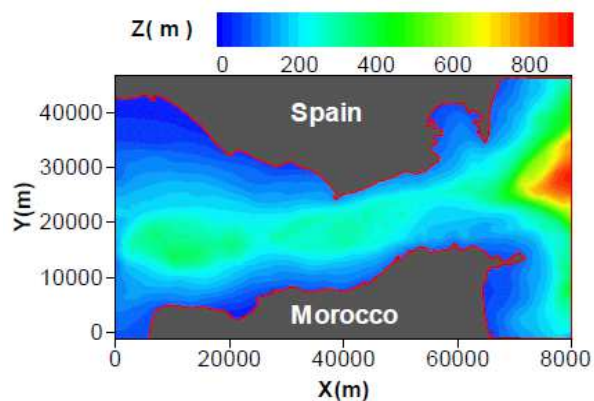


Fig. 12. Location and bathymetry of the strait of Gibraltar.

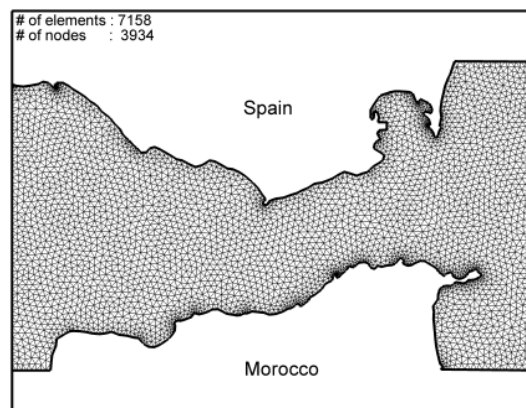


Fig. 13. Bathymetries and mesh of the strait of Gibraltar.

3.2 Pollutant convection in strait of Gibraltar

The strait of Gibraltar is an arm of the sea dividing Europe from Africa, with a strait of just 13 km width separating the two continents. The system is about 60 km in length between Barbate-Tangier in the West and Gibraltar-Sebta in the East. Its width varies between a minimum of about 14 km from Tarifa to Punta Cires and a maximum of 44 km from Bar-bate to Tangier. To verify its validity, the RWPT method was used to simulate hypothetical pollutant transport during a typical tidal period. The main concern of this test was to display the capacity of RWPT to handle irregular topography and complex geometry, in comparison to the Eulerian method. Equation (1) was implemented to simulate the flow within the strait over a triangular mesh presented in Fig. 13, and equation (2) for simulating the transport of the pollutant. On other hand, particle tracking was used to simulate the same pollutant divided into a set of particles.

In this test we assume the pollutant flows with a constant diffusion coefficient $D_x = D_y = 0.001 \text{ m}^2/\text{s}$, The Manning coefficient is set to $n = 0.001 \text{ s}/\text{m}^{1/3}$. The bathymetry employed in our calculations is depicted in Fig. 12, the maximum depth in the selected area exceeds 1000 m. For the sake of stability, careful numerical treatment of bathymetry has been deployed to bypass major numerical difficulties such as the C-property [19].



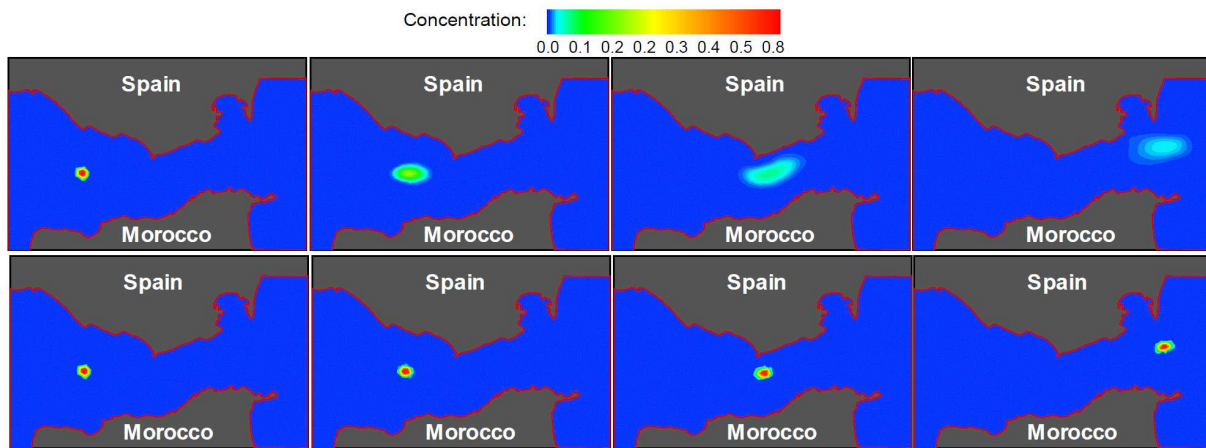


Fig. 14. Pollutant concentration calculated by the Eulerian convection diffusion equation (top row) and particle tracking method (bottom row) at different simulation times, from left to right $t=0, 2, 7.9$ and $12h$.

Initially, the water is at rest, and tidal forcing, with main astronomical tidal constituents M2, S2, and N2 [30], is used to generate the flow. Then, a pollutant plume with a maximal concentration of 1 is released and tracked, at the same time, with the RWPT method and solved by the convection-diffusion equation. Fig. 14 presents the numerical results. As plotted, the pollutant is propagated over the area by following the flow until the outlet of the computational zone. The maximum concentration, calculated by the Eulerian method decreases, contrary to the concentration of particle clouds simulated with RWPT which remains almost the same. It is intuitively obvious from the comparison of the two approaches that the RWPT approach overcomes spontaneously the numerical diffusion that affects the Eulerian methods. Besides, The RWPT method used for solute transport is independent of mesh.

Finally, The RWPT method is conservative because the mass of the tracer remains constant as the particles move in the domain and do not disappear. These properties prove that the RWPT is a better alternative to the convection-diffusion equation and useful for mass transport in water flows.

4. Conclusions

This paper has described the application of the shallow water equations coupled with the random particle tracking model to solve the convection-diffusion of pollutants in shallow water flow. This work is to improve the implementation of the model on a triangular mesh. The released particles are automatically controlled by the pollutant concentration and the particle density is used to manage the number of released particles. The validation is carried out using two test cases: with simple geometry with and without bathymetry and more complex bathymetry. First, this model is verified by solving a pollutant release problem in a uniform flow. The analytical solution is used as a reference. The results reveal several advantages of this RWPT method, including high accuracy, stability, and simplicity. The procedure used to calculate the pollutant concentration shows also high accuracy. Furthermore, the comparison of the obtained results by the RWPT with those by the Eulerian approach leads us to conclude that the particle tracking is free of the numerical diffusion and the maximum concentration is preserved when the displacement is governed by the advection process. Then, the robustness of the model and the capability of simulating flows in environments with complex geometries and bathymetry are demonstrated by a hypothetical pollutant transport problem in the strait of Gibraltar.

Author Contributions

Chaabelasri and Salhi planned, initiated the project; Jeyar and Chaabelasri developed mathematical and the numerical models, the implementation was assured by Hind Talbi. The manuscript was written through the contribution of all authors. All authors discussed the results, reviewed, and approved the final version of the manuscript.

Acknowledgments

We thank the two anonymous reviewers whose comments and suggestions helped improve and clarify this article.

Conflict of Interest

The authors declared no potential conflicts of interest with respect to the research, authorship, and publication of this article.

Funding

The authors received no financial support for the research, authorship, and publication of this article.

References

- [1] Paster, A., Bolster, D., Benson, D.A., Connecting the dots: Semi-analytical and random walk numerical solutions of the diffusion-reaction equation with stochastic initial conditions, *Journal of Computational Physics*, 263, 2014, 91–112.
- [2] Delay, F., Ackerer, P., Danquigny, C., Simulating solute transport in porous or fractured formations using random walk particle tracking A review, *Vadose Zone Journal*, 4(2), 2005, 360-379.
- [3] Majumder, P., Eldho, T.I., Vectorized simulation of groundwater flow and contaminant transport using analytic element method and random walk particle tracking, *Hydrological Processes*, 31(5), 2017, 1144–1160.
- [4] Scheidegger, A.E., Statistical hydrodynamics in porous media, *Journal of Geophysical Research*, 66, 1954, 3273–3278.



- [5] De Josselin de Jong, G., Longitudinal and transverse diffusion in granular deposits, *Transactions American Geophysical Union*, 39, 1958, 67–74.
- [6] Zhang, Z.A., Comparison of the Eulerian and Lagrangian methods for predicting particle transport in enclosed spaces, *Atmospheric Environment*, 41(25), 2007, 5236–5248.
- [7] Wu, X.F., Liang, D., Study of pollutant transport in depth averaged flows using random walk method, *Journal of Hydrodynamics*, 31(2), 2019, 303–316.
- [8] Park, C.H., Beyer, C., Bauer, S., Kolditz, O., Using global node-based velocity in random walk particle tracking in variably saturated porous media: Application to contaminant leaching from road constructions, *Environmental Geology*, 55(8), 2008, 1755–1766.
- [9] Selle, B., Rink, K., Kolditz, O., Recharge and discharge controls on groundwater travel times and flow paths to production wells for the Ammer catchment in southwestern Germany, *Environmental Earth Sciences*, 69(2), 2013, 443–452.
- [10] Bechtold, M., Vanderborght, J., Ippisch, O., Vereecken, H., Efficient random walk particle tracking algorithm for advective-dispersive transport in media with discontinuous dispersion coefficients and water, *Water Resources Research*, 47(10), 2011, W10526.
- [11] Ahmed, M.I., Abd-Elmegeed, M.A., Hassan, A.E., Modelling transport in fractured media using the fracture continuum approach, *Arabian Journal of Geosciences*, 12, 2019, 172.
- [12] LaBolle, E.M., Fogg, G.E., Tompson, A.F.B., Random-walk simulation of transport in heterogeneous porous media: local mass-conservation problem and implementation methods, *Water Resources Research*, 32(3), 1996, 583–593.
- [13] Masciopinto, C., Particles transport in a single fracture under variable flow regimes, *Advances in Engineering Software*, 35(5), 1999, 327–337.
- [14] Zhang, Z., Chen, Q., Comparison of the Eulerian and Lagrangian methods for predicting particle transport in enclosed spaces, *Atmospheric Environment*, 41(25), 2007, 5236–5248.
- [15] Cheng, K., Acevedo-Bolton, V., Jiang, R. et al. Stochastic modeling of short-term exposure close to an air pollution source in a naturally ventilated room: An autocorrelated random walk method, *Journal of Exposure Science and Environmental Epidemiology*, 24, 2014, 311–318.
- [16] Wu, X., Liang, D., Study of pollutant transport in depth-averaged flows using random walk method, *Journal of Hydrodynamics*, 31(2), 2019, 303–316.
- [17] Yang, F., Liang, D., Wu, X., Xiao, Y., On the application of the depth-averaged random walk method to solute transport simulations, *Journal of Hydroinformatics*, 22(1), 2020, 33–45.
- [18] Jalali, M.M., Borthwick, A.G.L., Tracer advection in a pair of adjacent side-wall cavities, and in a rectangular channel containing two groynes in series, *Journal of Hydrodynamics*, 30, 2018, 564–572.
- [19] Chaabelasri, E.M., Borthwick, A.G.L., Salhi, N., Elmahi, I., Balanced adaptive simulation of pollutant transport in bay of tangier, *World Journal of Modelling & Simulation*, 10(1), 2014, 3–19.
- [20] Chaabelasri, E., Jeyar, M., Salhi, N., Elmahi, I., A simple unstructured finite volume scheme for solving shallow water equations with wet/dry interface, *International Journal of Mechanical Engineering and Technology*, 10(1), 2019, 1849–1861.
- [21] Chaabelasri, E.M., Amahmouj, A., Jeyar, M., Borthwick, A.G.L., Salhi, N., Elmahi, I., Numerical survey of contaminant transport and self-cleansing of water in nador lagoon, Morocco, *Modelling and Simulation in Engineering*, 2014, 2014, 179504.
- [22] Liang, Q., Flood simulation using a well-balanced shallow flow model, *Journal of Hydraulic Engineering*, 136, 2010, 669–75
- [23] Li, G., Song, L., Gao, J., High order well-balanced discontinuous Galerkin methods based on hydrostatic reconstruction for shallow water equations, *Journal of Computational and Applied Mathematics*, 340, 2018, 546–560.
- [24] Xia, C., Cao, Z., Pender, G., Borthwick, A., Numerical algorithms for solving shallow water hydro sediment-morphodynamic equations, *International Journal for Computer Aided Engineering and Software*, 34(8), 2017, 2836–2861.
- [25] Hou, I., Wang, R., Liang, Q., Li, Z., Huang, M.S., Hinkelmann, R., Efficient surface water flow simulation on static Cartesian grid with local refinement according to key topographic features, *Computers and Fluids*, 176, 2018, 117–134.
- [26] Robinson, B.A., Dash, Z.V., Srinivasan, G., A Particle tracking transport method for the simulation of resident and flux-averaged concentration of solute plumes in groundwater models, *Computational Geosciences*, 14(4), 2014, 779–792.
- [27] Srinivasan, G., Keating, E., Moulton, J.D., Dash, Z.V., Robinson, B.A., Convolution based particle tracking method for transient flow, *Computational Geosciences*, 16(3), 2012, 551–563.
- [28] Salamon, P., Fernandez-Garcia, D., Gomez-Hernandez, J.J., A review and numerical assessment of the random walk particle tracking method, *Journal of Contaminant Hydrology*, 87(3–4), 2006, 277–305.
- [29] Lattanzi, A.M., Yin, X., Hrenya, C.M., A fully-developed boundary condition for the random walk particle tracking Method, *International Journal of Heat and Mass Transfer*, 131, 2019, 604–610.
- [30] Benkhaldoun, F., Elmahi, I., Seaid, M., Well-balanced finite volume schemes for pollutant transport by shallow water equations on unstructured meshes, *Journal of Computational Physics*, 226(1), 2017, 180–203.

ORCID iD

Talbli Hind  <https://orcid.org/0000-0003-1332-0081>

Chaabelasri Elmiloud  <https://orcid.org/0000-0003-2542-4021>

Jeyar Mohammed  <https://orcid.org/0000-0002-9052-2077>

Najim Salhi  <https://orcid.org/0000-0001-7840-613X>



© 2020 by the authors. Licensee SCU, Ahvaz, Iran. This article is an open access article distributed under the terms and conditions of the Creative Commons Attribution-NonCommercial 4.0 International (CC BY-NC 4.0 license) (<http://creativecommons.org/licenses/by-nc/4.0/>).

How to cite this article: Hind T., Elmiloud C., Mohammed J., Salhi N. Random Walk Particle Tracking for Convection-diffusion Dominated Problems in Shallow Water Flows, *J. Appl. Comput. Mech.*, 7(2), 2021, 486–495.
<https://doi.org/10.22055/JACM.2020.35154.2579>

